

# On the nonlinear stress-strain behavior of nematic elastomers - materials of two coupled preferred directions

A. M. Menzel<sup>1,a)</sup>, H Pleiner<sup>2,b)</sup>, and H. R. Brand<sup>1,2,c)</sup>

<sup>1)</sup> *Theoretische Physik III, Universität Bayreuth, 95440 Bayreuth, Germany*

<sup>2)</sup> *Max Planck Institute for Polymer Research, P.O. Box 3148, 55021 Mainz, Germany*

(Received 24 July 2008; accepted 11 November 2008; published online 5 January 2009)

We present a nonlinear macroscopic model in which nematic side-chain liquid single crystal elastomers are understood as materials that show two preferred directions. One of the two directions is connected to the director of the liquid crystalline phase, the other one becomes anchored in the polymer network during the procedure of synthesis. The specific properties of the materials arise from the coupling between these two preferred directions. We take into account this coupling via the variables of relative rotations between the two directions. For this purpose, we have extended the variables of relative rotations to the nonlinear regime. In addition, we generalize the concept in such a way that it can also be used for the description of other systems coupling two preferred directions. In order to test our picture, we compare its predictions to the experimental observations on nematic monodomain elastomers. As a result, we find that our model describes the nonlinear strain-induced director reorientation and the related plateau-like behavior in the stress-strain relation, which are characteristic of these materials. In addition, our model avoids the unphysical notion of a vanishing or small linear elastic shear modulus. Finally, we demonstrate that ordinary nonlinear elastic behavior of the materials, i.e. not connected to any reorientation of the director field, also plays an important role in the appearance of the stress-strain curves and must be taken into account. © 2009 American Institute of Physics. [DOI: 10.1063/1.3054295]

## I. INTRODUCTION

The first report of the synthesis of a monodomain nematic side-chain elastomer already contained a description of the most inspiring feature of these materials<sup>1,2</sup>: in nematic side-chain liquid single crystal elastomers (SCLSCEs) macroscopic deformation and reorientation of the nematic director field are closely connected. This fact was revealed when a nematic SCLSCe was stretched perpendicularly to its original director orientation in a stress-strain experiment. At the same time the orientation of the director field was traced by monitoring the dichroic ratio. The meantime well-known result was a continuous reorientation of the director field which set in at a threshold strain and appeared to be closely connected to a decrease in the slope of the stress-strain curve. In various later experiments this behavior of the materials was recovered. It was also found that the reorientation of the director can occur via a splitting of the homogeneous director orientation, when stripe domains are observed<sup>3,4</sup>. Furthermore, it was demonstrated that, vice versa, a reorientation of the director field causes macroscopic strain. This was shown by applying an external electric field to swollen nematic SCLSCEs<sup>5-7</sup>.

Since the early experiments have been performed, the topic is under thorough discussion from the point of view of modeling. In the previous decade the nonlinear elastic behavior has mainly been described using the semi-microscopic picture based on anisotropic Gaussian rubber elasticity<sup>8</sup>, which has

also been taken as a basis for numerical studies<sup>9</sup>. This approach is able to describe the plateau-like feature in the stress-strain curve at finite strains, where the director rotates from a perpendicular to a parallel orientation w.r.t. the stretching direction. In this approach there is no nematic degree of freedom considered and the nematic ordering simply serves as providing the uniaxial orientation. The rubber elastic description is based on the assumption of Gaussian phantom chains and affine deformations on all length scales. This approach, however, fails to correctly describe the linear elastic properties of nematic SCLSCEs. It predicts a vanishing (“soft”) or very small (“semi-soft”) linear elastic shear modulus, while oscillating shear measurements clearly show the shear elastic modulus to be finite and of the order of the isotropic one<sup>10-12</sup>. The linear “softness” has been linked to a spontaneously broken continuous shape rotational symmetry<sup>13</sup>. This symmetry is not spontaneously broken in the nematic SCLSCEs available experimentally so far.

Recently, a biaxial model has been proposed<sup>14</sup> to describe the results of the nonlinear stress-strain experiments. The two directions in the nematic SCLSCe are assumed to be given on the one hand by an internal stress imprinted into the material during the process of synthesis, and on the other hand by the external stress applied to the material during the stress-strain experiment. Here, the critical behavior is shifted from the linear elastic range to that of a finite strain thereby mimicking the nonlinear elastic plateau. However, no vanishing linear elastic shear modulus has been found experimentally even at a finite pre-strain.

Thus, there is a clear necessity for a description that cov-

<sup>(a)</sup>Electronic mail: andreas.menzel@uni-bayreuth.de

<sup>(b)</sup>Electronic mail: pleiner@mpip-mainz.mpg.de

<sup>(c)</sup>Electronic mail: brand@uni-bayreuth.de

ers the nonlinear plateau behavior as well as the non-soft (finite) linear shear elastic property. This could be provided by a more refined semi-microscopic model or by a macroscopic, phenomenological approach according to generalized hydrodynamics. The former has been discussed in Refs. 15 and 16, while the latter will be pursued below.

The picture that we propose in this paper is the following. We think of the materials as being composed of two components that both show a preferred direction. These two components are coupled to each other: a rotation of one of the two components with respect to the other one contributes to the energy density of the whole system. In our case of nematic SCLSCes, one of the two components is made up by the entity of mesogens that show the liquid crystalline phase. The other component is given by the crosslinked network of polymer backbones which shows an elastic mechanical behavior. Both of the two components feature a preferred direction, generally in parallel orientation in equilibrium. In our model these two directions are internal properties of the materials, which makes a major difference compared to the picture in Ref. 14.

Our concept is based on an early idea by de Gennes, who set up a linear expression for the variables of relative rotations between the director of the liquid crystalline phase and the polymer network<sup>17</sup>. Later on, relative rotations have been introduced as macroscopic variables into a hydrodynamic description of nematic SCLSCes by two of the present authors<sup>18</sup>. The concept of relative rotations has since turned out to be very useful in the macroscopic characterization of the materials<sup>11,12,19-21</sup>. Recently, we have extended the expression of relative rotations to the nonlinear regime, so that now also the nonlinear behavior of nematic SCLSCes can be modeled in this spirit<sup>22</sup>. Our characterization is macroscopic and can be understood as a starting point for a hydrodynamic description of the materials. We keep it general in the sense that we do not assign specific values to the material parameters from the beginning. Therefore it essentially differs from the approach given in Ref. 8. We will focus our considerations on the effects connected to the coupling of the two preferred directions in the elastomers. This coupling and relative rotations between the two preferred directions can lead to a strongly nonlinear response during stress-strain measurements. In particular, this response is not connected to the nonlinear purely elastic response that can be found for the materials in a strain-regime where no rotation of the preferred directions occurs. The analysis of experimental results corroborates our concept.

Possible applications of liquid crystalline elastomers as components of artificial muscles or soft mechanical actuators have been discussed in the literature<sup>5,23-25</sup>. The effect that we study in this paper may be exploited for practical purposes in the following way. As we have mentioned above, the reorientation of the director of common nematic SCLSCes can be initiated by stretching the respective elastomer perpendicularly to its initial director orientation, beyond a certain threshold value. While the director reorientation takes place, the slope of the corresponding stress-strain curve is strongly decreased. This means that then, by small changes of the amplitude of the applied stress, large changes of the elongation

of the material can be achieved. The respective SCLSCe therefore serves as a shape changing device that reacts very sensitively to variations of the externally applied stress. To drive the elastomer into this stress-sensitive regime, a pre-strain has to be imposed. We note at this point that the initiation of large amplitudes of deformation has also been reported for other kinds of materials under pre-strain<sup>26</sup>. On the other hand, nature has already been making use of the special properties of macromolecular materials containing liquid crystalline components for millions of years. A prominent example concerns the process of spinning fibers by spiders, which is connected to the partial liquid crystalline composition of spider silk<sup>27</sup>. Spider silk itself also features regimes of stress-sensitive behavior under elevated temperature and/or relative humidity, when the overall shape of the corresponding stress-strain curves is considered<sup>28</sup>.

We have organized this paper in the following way. In Sec. II we will describe in detail our nonlinear picture of nematic SCLSCes as materials of two coupled preferred directions. The elements of our previous nonlinear study of the materials will shortly be reviewed and implemented into the description. We give an expression for the generalized energy density of the system and discuss the various contributions. Furthermore, we show that in the linear regime de Gennes' picture of the materials is recovered. After that, in Sec. III we present the predictions of our model and compare them to experimental observations in the field. In particular, we focus on the results obtained during recent stress-strain experiments<sup>29,30</sup>. Finally, we summarize and discuss our results and give a short perspective in Sec. IV. We have added an appendix in which an alternative approach to the variables of relative rotations is presented. In addition, in the appendix we demonstrate that this alternative approach leads to an identical description of the materials when the corresponding terms of the generalized energy density are investigated.

## II. MACROSCOPIC MODEL OF NEMATIC SCLSCES

In this section we present in detail the ingredients of our model describing the macroscopic physical behavior of nematic SCLSCes. As we have already explained in Sec. I, in our picture the materials can be thought of as a combination of two coupled components. Each of these two components is associated with one preferred direction.

The preferred direction connected to the component showing the liquid crystalline phase is of course given by the director field  $\hat{\mathbf{n}}(\mathbf{r})$ . It reflects the average direction of orientation of the mesogenic units in a mesoscopic volume at a position  $\mathbf{r}$ . During strain-induced reorientation processes at constant temperature, it has been observed that within domains of one orientation of the director, the scalar order parameter  $S$  is either slightly decreasing or constant within the experimental error bar<sup>3</sup>. Due to this fact, we will not take into account the scalar degree of ordering  $S$  of the mesogens, but only deal with the orientation of the macroscopic director field.

On the other hand, we can identify a separate, second preferred direction which is connected to the polymer network,

or, in our language, to the component showing the elastic behavior. If the director of a nematic SCLSCE is reoriented during a stress-strain experiment or due to an external electric or magnetic field, it will relax back to its original orientation after the external force has been released. The original orientation of the director has been imprinted into the polymer network during the process of synthesis, or, in other words, it has been frozen in<sup>31</sup>. For materials generated by the two-step crosslinking procedure described in Refs. 1 and 2, it is easy to identify this direction: during a second crosslinking step the material is stretched in a certain direction in order to macroscopically align the director in a monodomain across the whole elastomer. It has been demonstrated that during the second crosslinking step some anisotropy gets locked in the vicinity of the crosslinking points<sup>2</sup>. But also if the director is macroscopically aligned by an external magnetic field<sup>32</sup>, by anisotropic deswelling<sup>33</sup>, or by surface effects<sup>34</sup> before the crosslinking process is completed, the respective original orientation of the director field becomes imprinted into the polymer network. We therefore identify this imprinted direction as the preferred direction of the network of polymer backbones, which makes up the second component. We denote this direction by  $\hat{\mathbf{n}}^{\text{nw}}(\mathbf{r})$ .

Due to the coupling between the two components it is clear that a misalignment of the two orientations  $\hat{\mathbf{n}}(\mathbf{r})$  and  $\hat{\mathbf{n}}^{\text{nw}}(\mathbf{r})$  will contribute to the generalized energy density of the system. From this misalignment, we will therefore construct nonlinear macroscopic variables which are suitable for a macroscopic, hydrodynamic-like description of the systems. Our scope in this section is to derive an expression for the generalized energy density characterizing the behavior of the materials.

It is important that the macroscopic variables that contribute to a hydrodynamic picture vanish when the system is in equilibrium and no external forces are applied. We take the difference between the two directions  $\hat{\mathbf{n}}(\mathbf{r}) - \hat{\mathbf{n}}^{\text{nw}}(\mathbf{r})$  as a starting point, however, it cannot be taken directly as the macroscopic variables we are looking for due to the following reasons of symmetry.

In low molecular weight nematics the two directions  $\hat{\mathbf{n}}(\mathbf{r})$  and  $-\hat{\mathbf{n}}(\mathbf{r})$  cannot be distinguished. Therefore, an expression for the generalized energy density characterizing such a system must be invariant under the symmetry transformation  $\hat{\mathbf{n}}(\mathbf{r}) \leftrightarrow -\hat{\mathbf{n}}(\mathbf{r})$ . For this reason, when deriving an expression for the generalized energy density, it makes sense to use macroscopic variables that show a clear behavior of symmetry under the transformation  $\hat{\mathbf{n}}(\mathbf{r}) \leftrightarrow -\hat{\mathbf{n}}(\mathbf{r})$ .

Returning to nematic SCLSCEs, we have two separate preferred directions  $\hat{\mathbf{n}}(\mathbf{r})$  and  $\hat{\mathbf{n}}^{\text{nw}}(\mathbf{r})$ . The generalized energy density must be invariant under the symmetry transformation  $\hat{\mathbf{n}}(\mathbf{r}) \leftrightarrow -\hat{\mathbf{n}}(\mathbf{r})$  as well as under the symmetry transformation  $\hat{\mathbf{n}}^{\text{nw}}(\mathbf{r}) \leftrightarrow -\hat{\mathbf{n}}^{\text{nw}}(\mathbf{r})$ , separately (inversion of  $\hat{\mathbf{n}}(\mathbf{r})$  does not imply inversion of  $\hat{\mathbf{n}}^{\text{nw}}(\mathbf{r})$  and vice versa). Our macroscopic variables must show a definite behavior under these transformations of symmetry.

We thus define two sets of nonlinear relative rotations on the basis of the difference  $\hat{\mathbf{n}}(\mathbf{r}) - \hat{\mathbf{n}}^{\text{nw}}(\mathbf{r})$ . Taking the component of this difference that is perpendicular to  $\hat{\mathbf{n}}^{\text{nw}}(\mathbf{r})$ , we obtain

as variables of relative rotations

$$\tilde{\Omega}(\mathbf{r}) := \hat{\mathbf{n}}(\mathbf{r}) - [\hat{\mathbf{n}}(\mathbf{r}) \cdot \hat{\mathbf{n}}^{\text{nw}}(\mathbf{r})] \hat{\mathbf{n}}^{\text{nw}}(\mathbf{r}). \quad (1)$$

$\tilde{\Omega}(\mathbf{r})$  is odd under the transformation  $\hat{\mathbf{n}}(\mathbf{r}) \leftrightarrow -\hat{\mathbf{n}}(\mathbf{r})$  and even under the transformation  $\hat{\mathbf{n}}^{\text{nw}}(\mathbf{r}) \leftrightarrow -\hat{\mathbf{n}}^{\text{nw}}(\mathbf{r})$  (we mark the scalar product by “.”). Systematically taking the component of  $\hat{\mathbf{n}}(\mathbf{r}) - \hat{\mathbf{n}}^{\text{nw}}(\mathbf{r})$  which is perpendicular to  $\hat{\mathbf{n}}(\mathbf{r})$ , we obtain as a second set of variables of relative rotations

$$\tilde{\Omega}^{\text{nw}}(\mathbf{r}) := -\hat{\mathbf{n}}^{\text{nw}}(\mathbf{r}) + [\hat{\mathbf{n}}(\mathbf{r}) \cdot \hat{\mathbf{n}}^{\text{nw}}(\mathbf{r})] \hat{\mathbf{n}}(\mathbf{r}). \quad (2)$$

$\tilde{\Omega}^{\text{nw}}(\mathbf{r})$  is even under the transformation  $\hat{\mathbf{n}}(\mathbf{r}) \leftrightarrow -\hat{\mathbf{n}}(\mathbf{r})$  and odd under the transformation  $\hat{\mathbf{n}}^{\text{nw}}(\mathbf{r}) \leftrightarrow -\hat{\mathbf{n}}^{\text{nw}}(\mathbf{r})$ . Later we will comment on the role of the two sets of relative rotations, and we will show that this formulation is in accordance with the linear description in the spirit of de Gennes<sup>17</sup>.

As a next step, we must connect the orientations of  $\hat{\mathbf{n}}(\mathbf{r})$  and  $\hat{\mathbf{n}}^{\text{nw}}(\mathbf{r})$  to those variables which characterize the current macroscopic state of the system<sup>22</sup>. In our model, the state of a nematic SCLSCE is completely defined by the orientation of the director field  $\hat{\mathbf{n}}(\mathbf{r})$  and by the state of elastic distortion of the polymer network. Elastic distortions are described in terms of gradients of a displacement field  $\mathbf{u}(\mathbf{r})$  in the framework of elasticity theory<sup>35</sup>.

In order to include the energy density resulting from elastic distortions into our expression for the generalized energy density of the system, we will have to use the nonlinear strain tensor in the Euler notation<sup>36</sup>. The components of this strain tensor written in components of  $\mathbf{u}(\mathbf{r})$  read

$$\varepsilon_{ij} = \frac{1}{2} [\partial_i u_j + \partial_j u_i - (\partial_i u_k)(\partial_j u_k)]. \quad (3)$$

This tensor describes, how the distance between two volume elements of the elastomer changes during an elastic deformation. The spatial dependence on  $\mathbf{r}$  is not explicitly displayed in the following.

When we want to connect the preferred direction of the elastic component  $\hat{\mathbf{n}}^{\text{nw}}$  to the elastic deformation, we start with the original, undistorted state of the system. Here, we find that the two macroscopic preferred directions are aligned in parallel directions. We denote them as  $\hat{\mathbf{n}}_0$  and  $\hat{\mathbf{n}}_0^{\text{nw}}$ , respectively. Locally, due to some external force acting onto the system, the director  $\hat{\mathbf{n}}$  is obtained from  $\hat{\mathbf{n}}_0$  via a rotation  $\mathbf{S}^{22}$ ,

$$\hat{\mathbf{n}} = \mathbf{S} \cdot \hat{\mathbf{n}}_0. \quad (4)$$

In the same way, also  $\hat{\mathbf{n}}^{\text{nw}}$  is obtained from  $\hat{\mathbf{n}}_0^{\text{nw}}$  via a rotation which we denote as  $\mathbf{R}^{-1}$ ,

$$\hat{\mathbf{n}}^{\text{nw}} = \mathbf{R}^{-1} \cdot \hat{\mathbf{n}}_0^{\text{nw}}. \quad (5)$$

The rotation matrix  $\mathbf{R}^{-1}$  is connected to the local elastic distortion of the polymer network. This is due to the fact that every elastic distortion can be separated into a rotation and a pure strain deformation. We have derived an expression for

$\mathbf{R}^{-1}$  in Eq. (13) of Ref. 22, which reads

$$\begin{aligned} (R^{-1})_{ij} &= \delta_{ij} + \varepsilon_{ij} + \frac{3}{2}\varepsilon_{ik}\varepsilon_{kj} + \frac{5}{2}\varepsilon_{ik}\varepsilon_{kl}\varepsilon_{lj} - \varepsilon_{ik}\partial_k u_j \\ &+ \frac{35}{8}\varepsilon_{ik}\varepsilon_{kl}\varepsilon_{lm}\varepsilon_{mj} - \partial_i u_j - \frac{3}{2}\varepsilon_{ik}\varepsilon_{kl}\partial_l u_j \\ &- \frac{5}{2}\varepsilon_{ik}\varepsilon_{kl}\varepsilon_{lm}\partial_m u_j + \mathcal{O}((\nabla\mathbf{u})^5). \end{aligned} \quad (6)$$

Thus Eqs. (3), (5) and (6) connect  $\hat{\mathbf{n}}^{\text{nw}}$  to the displacement field  $\mathbf{u}$ .

At the beginning of this section we have taken the misalignment  $\hat{\mathbf{n}}^{\text{nw}} - \hat{\mathbf{n}}$  as a starting point for the construction of the variables of relative rotations. Eqs. (4) and (5) together with the condition  $\hat{\mathbf{n}}_0^{\text{nw}} \parallel \hat{\mathbf{n}}_0$  will guarantee rotational invariance with respect to the initial state of the system, when we set up the expression for the generalized energy density.

In the following, using symmetry arguments, we derive this expression for the generalized energy density of the system. The macroscopic variables that can contribute to the generalized energy density comprise the hydrodynamic variables of mass density  $\rho$ , density of momentum  $\mathbf{g}$ , and density of entropy  $\sigma$ , as well as the macroscopic variables of strain (3), relative rotations (1) and (2), and gradient fields like  $\nabla\hat{\mathbf{n}}$ . We combine these variables satisfying the symmetry requirements for an energy density, such as invariance under parity and under the transformations  $\hat{\mathbf{n}}^{\text{nw}} \leftrightarrow -\hat{\mathbf{n}}^{\text{nw}}$  and  $\hat{\mathbf{n}} \leftrightarrow -\hat{\mathbf{n}}$ , separately. In addition, we assume that for the investigation of the stress-strain geometry the strains  $\varepsilon$  and the relative rotations  $\tilde{\Omega}$  and  $\tilde{\Omega}^{\text{nw}}$  play the dominant role. Therefore, only terms composed of  $\varepsilon$ ,  $\tilde{\Omega}$ , and  $\tilde{\Omega}^{\text{nw}}$  are taken into consideration. The expression for the generalized energy density we want to study in the following amounts to

$$\begin{aligned} F &= c_1 \varepsilon_{ij}\varepsilon_{ij} + \frac{1}{2}c_2 \varepsilon_{ii}\varepsilon_{jj} \\ &+ \frac{1}{2}D_1 \tilde{\Omega}_i \tilde{\Omega}_i + D_1^{(2)} (\tilde{\Omega}_i \tilde{\Omega}_i)^2 + D_1^{(3)} (\tilde{\Omega}_i \tilde{\Omega}_i)^3 \\ &+ D_2 n_i \varepsilon_{ij} \tilde{\Omega}_j + D_2^{nw} n_i^{nw} \varepsilon_{ij} \tilde{\Omega}_j^{nw} \\ &+ D_2^{(2)} n_i \varepsilon_{ij} \varepsilon_{jk} \tilde{\Omega}_k + D_2^{nw,(2)} n_i^{nw} \varepsilon_{ij} \varepsilon_{jk} \tilde{\Omega}_k^{nw}, \end{aligned} \quad (7)$$

where summation over repeated indices is implied.

Here, the elastic behavior of the polymer network is assumed to be isotropic, as the first two terms indicate. We will comment on this point in section IV. The terms with the coefficients  $D_1$ ,  $D_1^{(2)}$ , and  $D_1^{(3)}$  include energetic contributions only related to relative rotations. For symmetry reasons, namely the required invariance under the transformations  $\hat{\mathbf{n}}^{\text{nw}} \leftrightarrow -\hat{\mathbf{n}}^{\text{nw}}$  and  $\hat{\mathbf{n}} \leftrightarrow -\hat{\mathbf{n}}$ , only even powers of the relative rotations may appear in these terms. Due to  $\tilde{\Omega}_i \tilde{\Omega}_i = \tilde{\Omega}_i^{nw} \tilde{\Omega}_i^{nw}$  we did not explicitly add the corresponding terms containing only the variable  $\tilde{\Omega}^{\text{nw}}$ . What comes next in expression (7) are the terms that couple the relative rotations to the strain of the elastomer. As we can see, the terms with the coefficients  $D_2$  and  $D_2^{nw}$  couple to the strain tensor in a linear way, whereas the terms with the coefficients  $D_2^{(2)}$  and  $D_2^{nw,(2)}$  couple to the strain tensor quadratically. An additional term

$\varepsilon_{ij}\varepsilon_{ij}\tilde{\Omega}_k\tilde{\Omega}_k$  can be included to model an effective change of the elastic coefficient  $c_1$  with increasing relative rotations between the director and the polymer network. However, we will not need this term for the following discussion. For all terms, strain is only included up to quadratic order. The motivation for this approach will become clear during Sec. III.

It is straightforward to demonstrate that in the linear regime of small strains and small relative rotations we recover de Gennes' expression for the energy density<sup>17</sup>. Taking only those terms from expression (7) which are quadratic in the macroscopic variables and substituting  $\hat{\mathbf{n}} = \hat{\mathbf{n}}_0 + \delta\mathbf{n}$  as well as  $\hat{\mathbf{n}}^{\text{nw}} = \hat{\mathbf{n}}_0^{\text{nw}} + \delta\mathbf{n}^{\text{nw}}$ , we obtain

$$\begin{aligned} F^{(lin)} &= c_1 \varepsilon_{ij}\varepsilon_{ij} + \frac{1}{2}c_2 \varepsilon_{ii}\varepsilon_{jj} \\ &+ \frac{1}{2}D_1 \tilde{\Omega}_i^{(lin)} \tilde{\Omega}_i^{(lin)} + \bar{D}_2 n_i \varepsilon_{ij} \tilde{\Omega}_j^{(lin)}. \end{aligned} \quad (8)$$

Here,  $\bar{D}_2 = D_2 + D_2^{nw}$  and  $\tilde{\Omega}^{(lin)} = \delta\mathbf{n} - \delta\mathbf{n}^{\text{nw}}$  (one has to take care of the parameterization in the case of antiparallel alignment of  $\hat{\mathbf{n}}_0$  and  $\hat{\mathbf{n}}_0^{\text{nw}}$ ). For isotropic elastic behavior, this expression of  $F^{(lin)}$  coincides with de Gennes' expression as noted in Ref. 17. We obtain the conditions of thermodynamic stability:  $c_1 > 0$ ,  $2c_1 + 3c_2 > 0$ ,  $D_1 > 0$ , and

$$4c_1 D_1 - \bar{D}_2^2 = 4c_1 D_1 - (D_2 + D_2^{nw})^2 > 0. \quad (9)$$

Furthermore, by construction, from Eqs. (1) and (2) it follows that

$$\hat{\mathbf{n}}^{\text{nw}} \cdot \tilde{\Omega} = 0, \quad \hat{\mathbf{n}} \cdot \tilde{\Omega}^{\text{nw}} = 0. \quad (10)$$

In the linear regime, this leads to the familiar condition  $\hat{\mathbf{n}} \cdot \tilde{\Omega}^{(lin)} = 0$ , or equivalently  $\hat{\mathbf{n}}^{\text{nw}} \cdot \tilde{\Omega}^{(lin)} = 0$ ,  $\hat{\mathbf{n}}_0 \cdot \tilde{\Omega}^{(lin)} = 0$ , and  $\hat{\mathbf{n}}_0^{\text{nw}} \cdot \tilde{\Omega}^{(lin)} = 0$ .

We have added an appendix, in which we outline an alternative approach to the variables of relative rotations. However, we can show that this alternative approach leads to the same terms listed in expression (7). In the appendix, we also discuss in detail the symmetry relations between  $\hat{\mathbf{n}}$  and  $\hat{\mathbf{n}}^{\text{nw}}$  connected to the distorted state of the elastomer, as well as  $\hat{\mathbf{n}}_0$  and  $\hat{\mathbf{n}}_0^{\text{nw}}$  connected to the undistorted state.

### III. PREDICTIONS OF THE MODEL AND COMPARISON TO EXPERIMENTAL RESULTS

In this section, we will analyze the geometry of stretching a nematic SCLSCE perpendicularly to its original director orientation using the model introduced above. We include a semi-quantitative comparison of the predictions of our model to the results obtained from the corresponding reorientation experiments. The main goal of this procedure is to reveal the dominating underlying processes that from a macroscopic point of view take place during the reorientation of the director field.

We begin by specifying the geometry, which is illustrated in Fig. 1. The  $z$ -direction of our Cartesian coordinate system

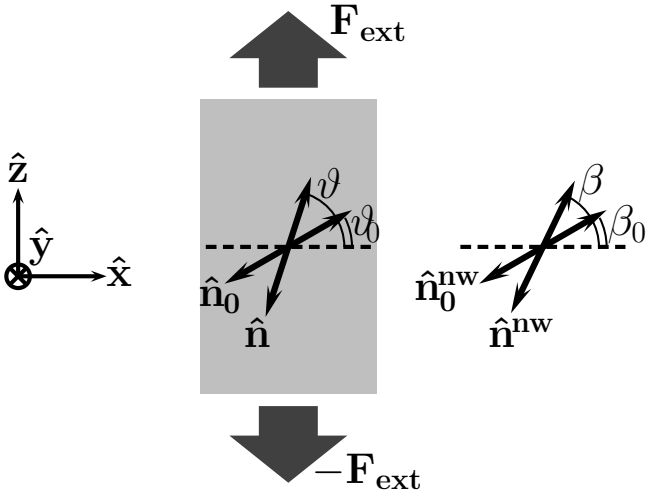


FIG. 1: Geometry of the system investigated. An external force  $\mathbf{F}_{\text{ext}}$  is applied parallel to the  $\hat{z}$  axis, the initial directions  $\hat{\mathbf{n}}_0$  and  $\hat{\mathbf{n}}_0^{\text{nw}}$  are oriented in the  $x$ - $z$ -plane. The angles between the  $\hat{x}$  axis and  $\hat{\mathbf{n}}_0$ ,  $\hat{\mathbf{n}}$ ,  $\hat{\mathbf{n}}_0^{\text{nw}}$ , and  $\hat{\mathbf{n}}^{\text{nw}}$  are called  $\vartheta_0$ ,  $\vartheta$ ,  $\beta_0$ , and  $\beta$ , respectively.

will be oriented parallel to the externally applied stretching force  $\mathbf{F}_{\text{ext}}$ . Furthermore, the initial directions  $\hat{\mathbf{n}}_0$  and  $\hat{\mathbf{n}}_0^{\text{nw}}$  are chosen to be oriented parallel within the  $x$ - $z$ -plane, so we can denote them as

$$\hat{\mathbf{n}}_0 = \begin{pmatrix} \cos \vartheta_0 \\ 0 \\ \sin \vartheta_0 \end{pmatrix}, \quad \hat{\mathbf{n}}_0^{\text{nw}} = \begin{pmatrix} \cos \beta_0 \\ 0 \\ \sin \beta_0 \end{pmatrix}, \quad (11)$$

with  $\vartheta_0 = \beta_0 + n\pi$ ,  $n \in \mathbb{Z}$ . When we set  $\vartheta_0 = 0$  we obtain the case of stretching the elastomer exactly perpendicularly to the original director orientation. Then  $\hat{\mathbf{n}}_0$  and  $\hat{\mathbf{n}}_0^{\text{nw}}$  are oriented parallel to the  $x$ -direction.

It is straightforward to study an inhomogeneous deformation and to include e.g. heterogeneous initial director orientations. However, in this paper we will adopt the assumption of a homogeneous deformation, which includes a homogeneous orientation of the initial directions  $\hat{\mathbf{n}}_0$  and  $\hat{\mathbf{n}}_0^{\text{nw}}$ . One should rather think of the homogeneous deformation of a characteristic volume element, not of the whole sample, a concept which we will further motivate later on.

In this spirit, we take as an ansatz for the displacement field

$$u_z = Az + Sx, \quad (12)$$

$$u_x = Bx + Tz, \quad (13)$$

$$u_y = Cy. \quad (14)$$

Here, the amplitudes  $A$ ,  $B$ ,  $C$ ,  $S$ , and  $T$  reflect the strain deformation of the elastomer. We know from the experiments that the reaction of the director field to the external forces is mainly determined by a reorientation within the  $x$ - $z$ -plane. Previous calculations in the spirit of our model show that within this plane the reorientation of the director is closely connected to a shear deformation of the elastomer<sup>11,22</sup>, as has also been found from other models. In ansatz (12)-(14), we therefore allow for a shear deformation in the  $x$ - $z$ -plane and discuss its role later.

We start our calculations by deriving an expression for the matrix  $\mathbf{R}^{-1}$ , which describes the elastic rotational deformation of the polymer network. For this purpose, we introduce ansatz (12)-(14) into Eqs. (3) and (6). Up to quartic order in the deformation amplitudes we obtain

$$\mathbf{R}^{-1} = \begin{pmatrix} \cos \bar{\beta} & 0 & -\sin \bar{\beta} \\ 0 & 1 + \mathcal{O}(C^5) & 0 \\ \sin \bar{\beta} & 0 & \cos \bar{\beta} \end{pmatrix}, \quad (15)$$

$$\bar{\beta} = (1 + \bar{A} + \bar{A}^2 + \bar{A}^3) \bar{S} - \left(\frac{1}{3} + \bar{A}\right) \bar{S}^3 + \mathcal{O}(5) \quad (16)$$

with  $\bar{\beta} \equiv \beta - \beta_0$ ,  $\bar{A} \equiv \frac{1}{2}(A + B)$  and  $\bar{S} \equiv \frac{1}{2}(S - T)$ . Here,  $\mathcal{O}(5)$  represents terms of quintic or higher order in the deformation amplitudes  $A$ ,  $B$ ,  $C$ ,  $S$ , and  $T$ .

We add four remarks. First, we see from Eqs. (15) and (16) that in the absence of any shear deformation (i.e.  $S = T = 0$ ) we do not find any elastic rotational deformation. The same is true for equal shear amplitudes  $S = T$ . Furthermore, in the linear regime we recover the fact that shear and rotational elastic deformations are equivalent:  $\beta - \beta_0 = -\frac{1}{2}(T - S)$ . Finally, only the shear amplitudes  $S$  and  $T$  determine the degree of elastic rotational deformation in the case of  $B = -A$  and  $C = 0$  (which is often referred to as a ‘‘pure shear’’ deformation; see, e.g., Ref. 38).

Using Eqs. (5), (15), and (16) we can now parameterize  $\hat{\mathbf{n}}^{\text{nw}}$  in terms of the deformation amplitudes. On the other hand, we have to include a further degree of freedom  $\vartheta$ , which is connected to the reorientation of the director  $\hat{\mathbf{n}}$  within the  $x$ - $z$ -plane. More precisely,  $\vartheta - \vartheta_0$  is denoting the angle by which the director has rotated from its original orientation  $\hat{\mathbf{n}}_0$  to its final orientation  $\hat{\mathbf{n}}$ . We obtain

$$\hat{\mathbf{n}} = \begin{pmatrix} \cos \vartheta \\ 0 \\ \sin \vartheta \end{pmatrix}, \quad \hat{\mathbf{n}}^{\text{nw}} = \begin{pmatrix} \cos \beta \\ 0 \\ \sin \beta \end{pmatrix}. \quad (17)$$

It is a very good approximation to assume that common nematic SCLSCs do not change their volume during the deformations investigated in the following. We include this feature by setting

$$C = \frac{-A - B + AB}{1 - A - B + AB}. \quad (18)$$

In particular, this expression for  $C$  implies that up to cubic order in the strain amplitudes the term with the coefficient  $c_2$  does not contribute to Eq. (7).

We can now obtain an expression for the energy density  $F$  which is a function only of the strain amplitudes  $A$ ,  $B$ ,  $C$ ,  $S$ , and  $T$ , as well as of the reorientation angle  $\vartheta$ . For this purpose, we have to introduce expressions (1)-(3), (12)-(14), and (16)-(18) into Eq. (7). We want to stress at this point that we will only take into account the strains up to quadratic order in the generalized energy density (7). The quadratic term of the strain tensor (3) enters  $F$  only in the terms with the coefficients  $D_2$  and  $D_2^{\text{nw}}$ , and Eq. (16) is reduced to  $\beta - \beta_0 = -\frac{1}{2}(T - S)$ . This way we make sure

that the nonlinear stress-strain behavior we will recover in the following originates solely from the influence of the relative rotations. There will be no terms included in the final form of expression (7) that can describe a nonlinear elastic behavior when no reorientation of the director occurs.

In our approach, we then have to minimize the generalized energy  $\mathcal{F} = \int_V F d^3r$  of the system,  $V$  being the volume of the respective sample. This means that we treat the system in a static way. We consider the respective elongation of the sample in  $z$ -direction to be imposed onto the system externally. Therefore, since we are dealing with a spatially homogeneous deformation, the value of the strain amplitude  $A$  is considered to be fixed from outside. For every value of  $A$  we determine the equilibrium state of the system.

Following this procedure, we have to minimize the generalized energy density  $F$  with respect to the strain amplitudes  $B$ ,  $C$ ,  $S$ , and  $T$ , as well as to the reorientation angle  $\vartheta$ . From this minimization we obtain the values of  $B$ ,  $C$ ,  $S$ ,  $T$ , and  $\vartheta$  as a function of  $A$ . Consequently, also the energy density  $F$  can be expressed as a function of  $A$ . From the change of the generalized energy density  $F$  with respect to  $A$ , that is from the derivative  $dF/dA$ , we can then deduce the value of the externally applied force  $F_{ext}$ .  $F_{ext}$  is connected to the external stress amplitude, and it is the cause of the respective elongation characterized by  $A$ . In this way our picture is closed.

Since we want to compare the results obtained from our model to experimental results, we should address two more issues before we start to evaluate the expression for  $F$ .

On the one hand, a completely spatially homogeneous deformation of the entire sample can of course not be realized in an experiment. This results already from the geometrical constraints connected to the respective experimental set-up, in interplay with the low compressibility of the materials. Especially near the top and bottom edges, where the samples are usually clamped during reorientation experiments, the strain deformation is quite heterogeneous. Because of this, a spatially homogeneous characterization can only describe the behavior of one volume element of the sample. Only if the geometry of the sample investigated is chosen such that most of the regions of the sample react in a similar way, and only if the behavior of a characteristic volume element can reflect the overall behavior of the sample, then this approach is meaningful.

Furthermore, for polymer materials it is difficult to map the overall boundary conditions of a clamped sample to one volume element. It seems plausible that shear deformations characterized by  $T \neq 0$  play a minor role. This is also suggested by the observations of the stripe domains, which are oriented parallel to the direction of the externally applied force<sup>3,4</sup>. As a consequence, we will set

$$T = 0 \quad (19)$$

during the rest of our considerations. The discussion is not as clear for shear deformations described by  $S \neq 0$ . Narrow stripes of alternating shear deformation  $S > 0$  and  $S < 0$ , respectively, do not lead to a large deviation from the boundary conditions imposed by the clamps. We will therefore study the

case of  $S = 0$  first, however, we will also discuss the influence of a nonvanishing shear deformation  $S \neq 0$ .

On the other hand, we have to connect the variables the values of which are measured during the experiments to the variables that appear in our hydrodynamic-like Eulerian picture. Usually, in the experiments the value of the current macroscopic dimension  $l$  of the respective sample in the direction of the externally applied force is recorded step by step. Comparing to the initial dimension  $l_0$  of the sample in this direction, the ratio

$$\lambda = \frac{l}{l_0} \quad (20)$$

is determined and taken as a measure of the induced strain. Sometimes, like for instance in Ref. 29, the so called true strain  $\epsilon = \ln(\lambda)$  is taken as a variable. We will choose our Cartesian coordinate system such that the externally applied force is oriented parallel to the  $z$ -direction (Fig. 1). Then,  $\lambda \equiv \lambda_z$ ,  $l \equiv l_z$ , and  $l_0 \equiv l_{z,0}$ . In the same way we define the current dimensions  $l_x$  and  $l_y$  as well as the initial dimensions  $l_{x,0}$  and  $l_{y,0}$  of the respective sample in the lateral directions. Stresses are recorded either as true stress

$$\sigma_{ext} = \frac{F_{ext}}{l_x l_y} \quad (21)$$

or as nominal stress

$$\sigma_{ext}^N = \frac{F_{ext}}{l_{x,0} l_{y,0}}, \quad (22)$$

where  $F_{ext}$  again denotes the magnitude of the force externally applied to the sample edges in  $z$ -direction. Underlying these definitions is, of course, the assumption that the sample deforms in a spatially homogeneous way. Naturally, from the experimental point of view the initial dimension  $l_0$  is considered to be constant and the current sample dimension  $l$  is changed.

In the hydrodynamic-like picture, however, the situation is different. Here, we have to adopt an Eulerian point of view. Therefore, the current dimension of the sample  $l$  is considered to be constant, and what changes is the initial dimension  $l_0$ .

Because of  $l_{z,0} = l_z - Al_z$ , in a spatially homogeneous deformation we obtain

$$\lambda = \frac{1}{1 - A}. \quad (23)$$

Furthermore, from

$$d\mathcal{F} = F_{ext} d(l_z - l_{z,0}) = -F_{ext} dl_{z,0} \stackrel{!}{=} l_x l_y l_z \frac{dF}{dA} dA \quad (24)$$

we find

$$\sigma_{ext} = \frac{F_{ext}}{l_x l_y} = \frac{dF}{dA}, \quad (25)$$

$$\sigma_{ext}^N = \frac{F_{ext}}{l_{x,0} l_{y,0}} = (1 - A) \frac{dF}{dA}. \quad (26)$$

Here, the expressions on the left of Eqs. (25) and (26) are given as functions of  $\lambda$ , the expressions on the right as

functions of  $A$ . The connection between both follows from Eq. (23).

In the following, we will continue our considerations in two steps. First, we will focus on the reorientation of the director field. In this context we can elucidate the different roles of the two sets of relative rotations. After that, we will address the stress-strain curves. We keep in mind that the reorientation of the director field and the nonlinear shape of the respective stress-strain curve are closely connected to each other.

### A. Reorientation of the director field

For illustration we will suppress shear elastic deformations in this subsection, that is we set  $S = T = 0$ . Therefore, no rotation of the polymer network occurs and  $\beta = \beta_0$ . Furthermore, we will only take into account the quadratic terms with the coefficients  $c_1, D_1, D_2, D_2^{nw}$ , as well as the term with the coefficient  $D_1^{(2)}$ . Only the linear components of the strain tensor (3) will be included in the beginning, so the strain tensor adopts the very simple form  $\varepsilon_{xx} = B, \varepsilon_{yy} = C, \varepsilon_{zz} = A$ , and  $\varepsilon_{ij} = 0$  for  $i \neq j$ .

As explained before, we then have to solve the system of equations  $dF/dB = dF/d\vartheta = 0$ . For the values of the material parameters, we choose  $c_1 = 121 \times 10^3 \text{ J m}^{-3}$ ,  $D_1 = 12 \times 10^3 \text{ J m}^{-3}$ ,  $D_2 = -32 \times 10^3 \text{ J m}^{-3}$ ,  $D_2^{nw} = -32 \times 10^3 \text{ J m}^{-3}$ , and  $D_1^{(2)} = 4.5 \times 10^3 \text{ J m}^{-3}$ . In general,  $c_1$  is obtained from the initial slope of the respective stress-strain curve before any reorientation of the director takes place. The choice of the other material parameters can be motivated in the following way. From a stability analysis for  $\vartheta_0 = 0^\circ$  we find that the original orientation of the director  $\vartheta = \vartheta_0 = 0^\circ$  becomes unstable at a critical strain given by  $A = A_c$ ,

$$A_c = -\frac{D_1}{2D_2 + D_2^{nw}}. \quad (27)$$

With increasing  $A > A_c$  the director continuously rotates and reaches an orientation of  $\vartheta = 90^\circ$  at  $A = A_r$ ,

$$A_r = A_c - \frac{8c_1 D_1^{(2)} - (D_2^{nw})^2}{2c_1(2D_2 + D_2^{nw})}. \quad (28)$$

For  $A > A_r$  the director remains at this orientation of  $\vartheta = 90^\circ$ .

We can infer from Eq. (27) that  $2D_2 + D_2^{nw} \stackrel{!}{<} 0$ , if a rotation of the director shall occur ( $D_1 > 0$ ). Furthermore, if the values of  $D_2$  and  $D_2^{nw}$  are set and the value of  $A_c$  is adopted from an experiment, we can estimate the value of  $D_1$ . On the contrary, estimate (28) has to be taken with care. The experiments show that the strain amplitudes corresponding to a complete reorientation of the director are rather high so that nonlinear effects will probably play a major role. Therefore, Eq. (28) should mainly be considered as an estimate for the order of magnitude of the value of  $D_1^{(2)}$ .

As a result, we obtain the curves depicted in Fig. 2, where the orientation angle of the director  $\vartheta$  is plotted against the

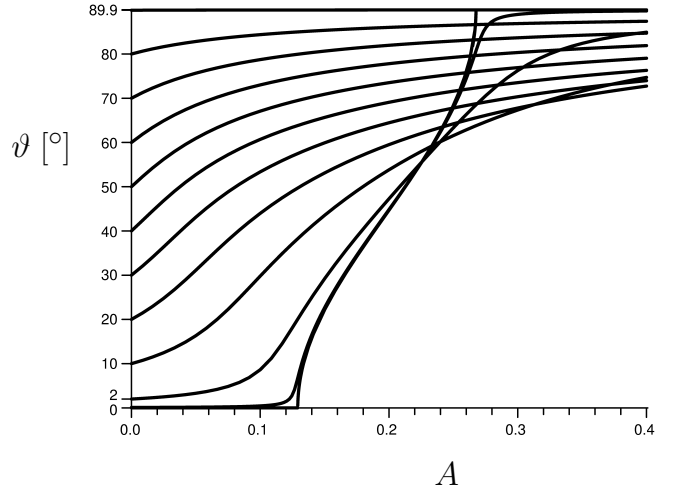


FIG. 2: Angle  $\vartheta$  between the director orientation and the  $\hat{\mathbf{x}}$  axis under the influence of an externally imposed strain  $A$ . The initial director orientations for  $A = 0$  were given by  $\vartheta(A = 0) = \vartheta_0 = 0^\circ, 0.1^\circ, 2^\circ, 10^\circ$  to  $80^\circ$  in steps of  $10^\circ$ , and  $89.9^\circ$ , respectively. They can be inferred from the scaling labels on the ordinate (the value  $\vartheta_0 = 0.1^\circ$  has not been marked explicitly). For  $\vartheta_0 = 0^\circ$  a pronounced threshold behavior is found.

externally imposed strain  $A$  (in the corresponding calculations the strain amplitudes have been taken into account up to quadratic order). The different curves correspond to different initial orientation angles  $\vartheta_0 = 0^\circ, 0.1^\circ, 2^\circ, 10^\circ$  to  $80^\circ$  in steps of  $10^\circ$ , and  $89.9^\circ$ , respectively, which can be inferred from the scaling labels on the ordinate (the value of  $\vartheta_0 = 0.1^\circ$  has not been marked explicitly). At small and large strain amplitudes the curves for  $\vartheta_0 = 0^\circ$  and  $\vartheta_0 = 0.1^\circ$  nearly coincide. Significantly, for an external force applied perfectly perpendicularly to the initial director orientation, that is for  $\vartheta_0 = 0^\circ$ , we find a pronounced threshold at a critical strain  $A_c \approx 0.13$ . However, the curve strongly smoothes out already for the small value of  $\vartheta_0 = 0.1^\circ$ . Naturally, when the director is already aligned parallel to the externally applied force ( $\vartheta_0 \approx 90^\circ$ ), practically no further reorientation occurs.

It is interesting to note that we find a complete alignment of the director parallel to the external force direction, that is  $\vartheta = 90^\circ$  at finite strains, only for the perfectly perpendicular geometry of  $\vartheta_0 = 0^\circ$ . In order to understand this point, we have a look at the terms with the coefficients  $D_2$  and  $D_2^{nw}$ , which induce the reorientation of the director field. For the geometry investigated, they read

$$D_2 n_i \varepsilon_{ij} \tilde{\Omega}_j + D_2^{nw} n_i^{nw} \varepsilon_{ij} \tilde{\Omega}_j^{nw} = D_2 n_x \varepsilon_{xx} \tilde{\Omega}_x + D_2^{nw} n_z^{nw} \varepsilon_{zz} \tilde{\Omega}_z^{nw} + D_2 n_z \varepsilon_{zz} \tilde{\Omega}_z + D_2^{nw} n_x^{nw} \varepsilon_{xx} \tilde{\Omega}_x^{nw}. \quad (29)$$

The first two terms after the equality sign are always positive, whereas the last two terms are always negative. This follows from definitions (1) and (2), as well as from  $\varepsilon_{xx} < 0$  and  $\varepsilon_{zz} > 0$ . In general, the energetic penalty arising from the first two terms in brackets inhibits a complete alignment of the director parallel to the external force direction. However, these terms vanish in a geometry in which the external stress

is always oriented perfectly perpendicular to  $\hat{\mathbf{n}}^{nw}$  ( $\vartheta_0 = 0^\circ$ ,  $S = T = 0$ ). More illustratively, we can say that the stretching of the elastomer given by  $\varepsilon_{zz} > 0$  enforces, whereas the induced contraction described by  $\varepsilon_{xx} < 0$  hinders the director reorientation via the relative rotations  $\tilde{\Omega}$ . The opposite is true for the role of the relative rotations  $\tilde{\Omega}^{nw}$ : here the stretching  $\varepsilon_{zz} > 0$  hinders and the induced contraction  $\varepsilon_{xx} < 0$  enforces the director reorientation. Only in the case of the perfectly perpendicular geometry without shear deformation, Eq. (29) only leads to contributions that drive the director to  $\vartheta = 90^\circ$ . In all the other cases additional contributions leading to the opposite effect arise. This is the reason for the very different appearances of the curves in Fig. 2.

For this special case of  $\vartheta_0 = 0^\circ$  and  $S = T = 0$ , we can also further elucidate the role of the two sets of relative rotations  $\tilde{\Omega}$  and  $\tilde{\Omega}^{nw}$ .  $\tilde{\Omega}$  directly couples to the externally imposed strain  $\varepsilon_{zz} = A$ , and this coupling induces the reorientation of the director field. On the other hand,  $\varepsilon_{zz} > 0$  results in a contraction  $\varepsilon_{xx} < 0$ , which couples to  $\tilde{\Omega}^{nw}$ . Then,  $\tilde{\Omega}^{nw}$  also enforces the director reorientation. Because of the coupling between  $\tilde{\Omega}^{nw}$  and  $\varepsilon_{xx}$ , however, the material parameter  $D_2^{nw}$  simultaneously influences the magnitude of the lateral contraction  $\varepsilon_{xx}$ .

When we want to compare the shape of the curves in Fig. 2 to the ones obtained during measurements, we have to rescale the abscissa via Eq. (23), introducing  $\lambda$  as a variable. This procedure stretches the shape of the curves for higher strains, a tendency which is also observed experimentally<sup>4</sup>. In our model, it is possible to fine-tune the shape of the curves especially for larger angles  $\vartheta$  via the values of the material parameters  $D_1^{(2)}$  and  $D_1^{(3)}$  (and using terms in the expression for  $F$  of even higher order in the relative rotations, if necessary). We note that for values  $D_1 > 0$ ,  $D_1^{(2)} < 0$ , and  $D_1^{(3)} > 0$  our model predicts a jump of the orientation angle  $\vartheta$  to higher values at a certain strain amplitude. A related behavior has been reported, for example, in Ref. 39.

## B. Stress-strain curves

In this section we will use our model in order to study the mechanical stress-strain behavior of nematic SCLSCes deformed in a geometry as described above. For this purpose we will compare the results of our model with data measured during recent stress-strain experiments.

We decided to focus on the stress-strain curve shown in Fig. 3. It was measured by Urayama et al. and it is reproduced from Fig. 5 of Ref. 29. The authors of Ref. 29 investigated a thin film of nematic SCLSCe of homeotropic ground state director alignment. At  $70^\circ\text{C}$  the film was deeply in the nematic state and showed a pronounced decrease in the slope of the stress-strain curve at intermediate strain amplitudes (Fig. 3). The reasons for us to focus on these data are of different kinds. For one thing, the data curve apparently represents a material which has sufficiently equilibrated for each step of increasing the strain. In particular, besides the stress-strain data also measurements revealing the orientation of the director field

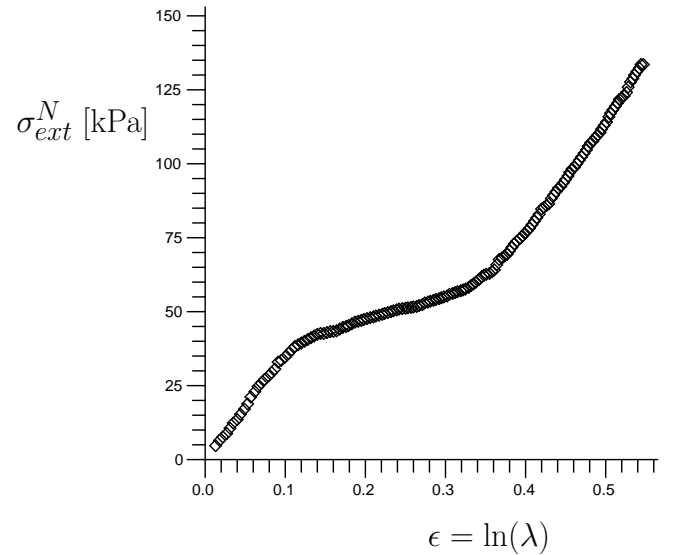


FIG. 3: Nominal stress  $\sigma_{ext}^N$  versus the true strain  $\epsilon = \ln(\lambda)$  measured for a nematic SCLSCe by Urayama et al. The data points were acquired for a thin film of homeotropic alignment at  $70^\circ\text{C}$  (reproduced from Fig. 5 of Ref. 29). Reprinted with permission from *Macromol.* **40**, 7665-7670 (2007). Copyright 2007 American Chemical Society.

as well as measurements on the dimensional shape change of the sample during the strain deformation are presented for the same material and thus give a complete picture.

Two important facts can be extracted from the region of high strain amplitudes in Fig. 3. We can see that the elastomer reacts in a well defined way to the imposed strain deformation. A fairly linear relationship has been found between the nominal stress  $\sigma_{ext}^N$  and the logarithm of the elongation  $\ln(\lambda)$  for these high strain amplitudes. This especially applies to the data points in the regime  $0.4 < \epsilon < 0.5$ . For  $\epsilon > 0.5$  the data points start to scatter and slightly deviate from this linear relationship. We interpret this fact as the onset of a qualitatively different behavior at very high strain amplitudes. Therefore we will restrict our considerations to the regime of  $\epsilon < 0.5$ . The authors of Ref. 29 could further demonstrate by infrared dichroism measurements that in the regime of high strain amplitudes ( $\epsilon > 0.4$ ) the director reorientation has been completed and practically no further reorientation occurs. Moreover, the slope of the stress-strain curve is roughly as large as for low strain amplitudes.

In order to compare with our model, we have to convert the stress-strain curve from Fig. 3 to the corresponding representation in terms of the variables  $A$  and  $dF/dA$ . We perform this step with the help of Eqs. (23) and (26). As a result, we obtain the curve depicted in Fig. 4.

Furthermore, we remember that in our approach we have derived the expression for the generalized energy density  $F$  by means of a series expansion in the strain tensor  $\varepsilon$ . As mentioned before, in our calculations pure elastic strain is explicitly included only to quadratic order. Nonlinear behavior of the stress-strain curve predicted by our expression for the generalized energy density  $F$  always has to be connected to a



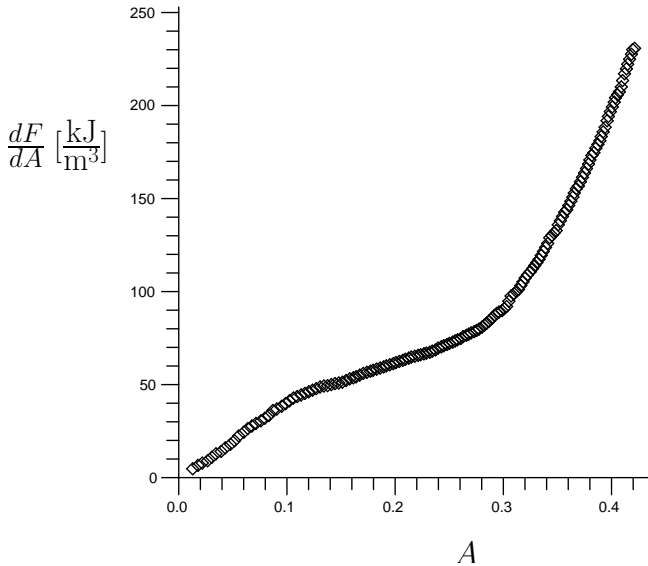


FIG. 4: Stress-strain data from Fig. 3 measured by Urayama et al. transferred to the representation in terms of  $A$  and  $dF/dA$ .

reorientation process of the director field. If the director orientation remains constant w.r.t. the polymer network, we will find a linear relationship between  $A$  and  $dF/dA$ .

A nonlinear behavior of the stress-strain curve in a regime of constant director orientation has to arise solely from an intrinsic nonlinear elastic behavior, resulting from stretching the network of crosslinked polymer backbones. We will subtract this nonlinear elastic behavior from the stress-strain curve. For this purpose we have fitted the linear regime of high strains in Fig. 3 by a straight line. With the help of Eqs. (23) and (26) we could transfer this straight line from the  $\ln(\lambda)$ - $\sigma_{ext}^N$  representation of Fig. 3 to the  $A$  -  $dF/dA$  representation of Fig. 4. We obtain  $dF/dA$  as a power series of  $A$ ,  $dF/dA = a_0 + a_1A + a_2A^2 + a_3A^3 + \dots$ . As mentioned above, the authors of Ref. 29 have demonstrated that for these high strain amplitudes no reorientation process of the director occurs. The nonlinear contributions in  $A$  must therefore result from nonlinear purely elastic contributions of the polymer network. Since these effects are not included in the characterization by our model, we can exclude them from our considerations: we subtract the values  $a_2A^2 + a_3A^3 + \dots$  from the data points of our stress-strain curve in the  $A$  -  $dF/dA$  representation. This is possible on the basis of our approach in the spirit of a series expansion, in which every effect is connected to a limited number of terms. As a result, we obtain the curve of data points shown by Fig. 5.

We have to note that, as a consequence of this procedure, we make a small error in the following sense. Terms, like for instance  $\varepsilon_{ij}\varepsilon_{jk}\varepsilon_{ki}\tilde{\Omega}_l\tilde{\Omega}_l$ , include the strain to higher than quadratic order and couple for example to relative rotations. At low strain amplitudes the term may vanish due to  $\tilde{\Omega} = \mathbf{0}$ . On the contrary, it may lead to a contribution nonlinear in  $A$  for higher strain amplitudes when  $\tilde{\Omega} = \mathbf{const} \neq \mathbf{0}$ . In this case, we may subtract the nonlinear influence of this term from the  $A$  -  $dF/dA$  curve only for the higher strain ampli-

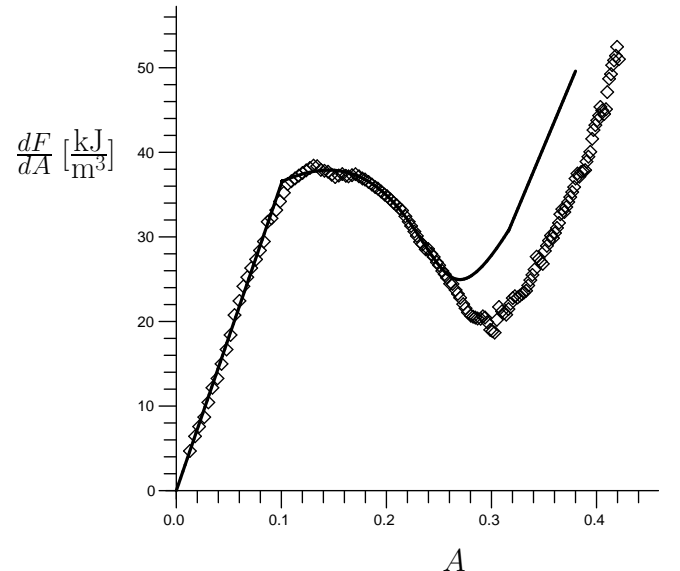


FIG. 5: Same stress-strain data as in Fig. 4 with nonlinear purely elastic contributions by the network of polymer backbones subtracted. A curve that has been obtained with the help of our model is also shown. In this case, the amplitude  $S$  of the shear deformation was free to adjust. The curve is characterized by a specific set of values of the material parameters involved in our model.

tudes where  $\tilde{\Omega} = \mathbf{const} \neq \mathbf{0}$ , not for the lower strain amplitudes of  $\tilde{\Omega} = \mathbf{0}$ . However, we have checked that the error resulting from these deviations are only minor. For this purpose, we have repeated the whole procedure, now fitting the linear regime of small strains of the  $\ln(\lambda)$ - $\sigma_{ext}^N$  plot with a straight line. Eventually, after subtracting the elastic nonlinearities resulting from this regime, we obtained almost the same curve as before. In short: we have verified that our procedure of fitting the original stress-strain curve leads essentially to the same results for both regimes, small and large amplitudes of strain.

As a first step in order to investigate the stress-strain behavior, we suppressed elastic shear deformations completely by setting  $S = T = 0$ . This means that  $\hat{\mathbf{n}}^{\text{nw}} \parallel \hat{\mathbf{n}}_0^{\text{nw}}$  during the whole deformation. We solve the equations  $dF/dB = dF/d\vartheta = 0$ , and we obtain  $B$  and  $\vartheta$  as a function of  $A$ . As a result, by choosing appropriate values for the material parameters, we obtain curves for  $dF/dA$  as a function of  $A$ , which qualitatively correspond to the arrangement of the data points in Fig. 5. When we choose  $\vartheta_0 = 0^\circ$  for the angle of initial director orientation, corresponding to  $\hat{\mathbf{n}}^{\text{nw}} \parallel \hat{\mathbf{x}}$ , we find pronounced cusps in the  $A$  -  $dF/dA$  curve. These cusps are located at the strain amplitudes where the director orientation starts and ends. They correspond to the kinks in the curve of  $\vartheta_0 = 0^\circ$  in Fig. 2. It is not surprising that such a threshold behavior occurs in the perfectly perpendicular geometry. We could demonstrate that a pretilt in the initial director orientation ( $\vartheta_0 \neq 0^\circ$ ) smoothes out the stress-strain curves. Simultaneously, however, it leads to an increase of the slope in the intermediate strain region. Spatial heterogeneities of the materials will also play a major role in this context. They

correspond to a spatial variation of the values of the material parameters in our model. As a qualitative estimate, we took simple averages over stress-strain curves obtained for different values of only one material parameter. The result indicates that the curves will be strongly smoothed under the influence of spatial variations.

Comparing the curves obtained in this way for  $S = 0$  to the data points, there is a major difference: the length of the interval of negative slope cannot be quantitatively reproduced. The reasons for this fact may comprise additional effects induced by spatial heterogeneities, which then would have to be included in our model. Furthermore, nonlinear contributions not considered up to now (such as, for example, described by higher order coupling terms of strain and relative rotations) can extend the width of the interval. However, the suppression of the shear deformation by setting  $S = 0$  also plays a major role, as will be demonstrated in the following.

### C. Including shear deformations

When we want to inspect the situation of  $S \neq 0$ , we have to solve the system of equations given by  $dF/dB = dF/dS = dF/d\vartheta = 0$ . As a result we obtain  $B$ ,  $S$ , and  $\vartheta$  as a function of  $A$ , noting that the corresponding algebra becomes quite complex. We have investigated the situation of an initial director orientation given by  $\vartheta_0 = 0^\circ$ . Here, we find that the threshold strain at which the director reorientation starts shifts to a lower value. Significantly, the strain interval over which the director reorientation takes place becomes considerably longer when the shear amplitude  $S$  is free to adjust. An example for the stress-strain curves we obtain by this procedure is shown in Fig. 5. The shear amplitude  $S$  connected to the corresponding deformation is depicted in Fig. 6. We can see that no shear deformation occurs below threshold. When the threshold strain amplitude has been passed and the director starts to reorient, the shear deformation steeply increases. It steeply decreases again when the reorientation angle of the director comes close to  $90^\circ$ . In the reoriented state we find no shear deformation, as it was the case for the low strain amplitudes.

We have plotted the evolution of the strain amplitude  $B$  corresponding to the resulting contraction in  $x$ -direction in Fig. 7. This is the direction parallel to the original orientations  $\hat{\mathbf{n}}_0$  and  $\hat{\mathbf{n}}_0^{nw}$ . The dependence of the amplitude  $B$  on the externally imposed strain  $A$  reflects well the experimental observations<sup>29</sup>. For low strain amplitudes  $A < A_c$  we obtain the linear isotropic elastic behavior of an incompressible material, characterized by  $B = -\frac{1}{2}A$ . As soon as the director reorientation sets in, however, this behavior changes qualitatively. We find that during the reorientation of the director field the lateral contraction mainly occurs in  $x$ -direction and can be described approximately by  $B \approx -A$ . This means that the elastic deformation occurs mainly in the plane of the director reorientation. Consequently, the material in this regime reacts approximately in a two dimensional way, which agrees well with the experimental observation<sup>5,29</sup>. This kind of deformation is often referred to as a ‘‘pure shear’’ deformation<sup>38</sup>. When the reorientation process has been completed, we again

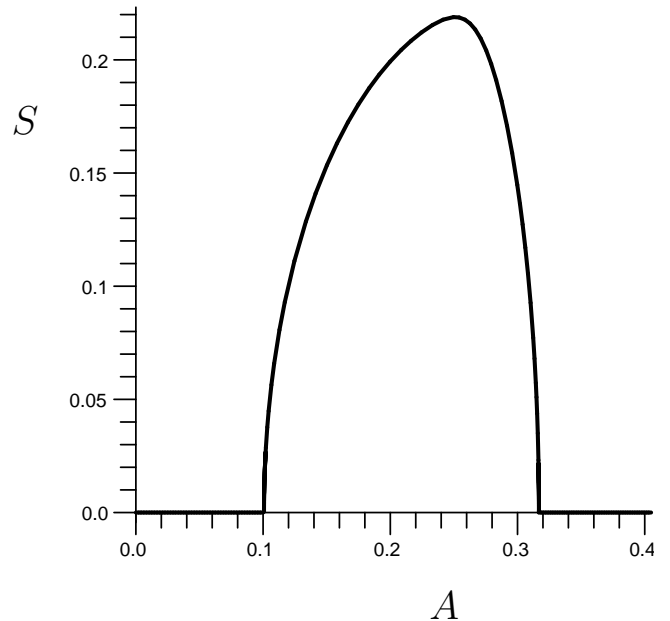


FIG. 6: Shear deformation of a volume element exposed to a strain  $A$ , during which the shear amplitude  $S$  is free to adjust.

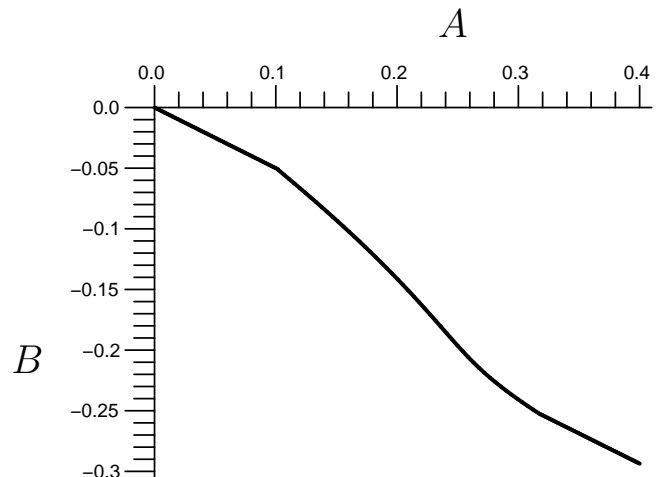


FIG. 7: Amplitude  $B$  describing the lateral contraction of a volume element exposed to a strain  $A$ , where the shear amplitude  $S$  is free to adjust.

find a behavior close to  $B = -\frac{1}{2}A$ . We would like to stress at this point that the respective magnitudes of the lateral contractions for  $A > A_c$  are mainly determined by the influence of the relative rotations  $\tilde{\Omega}^{nw}$ . When this second set of relative rotations is neglected, the elastic behavior of the materials is not recovered correctly.

In order to obtain the curves presented in Figs. 5-7, the values of the material parameters have been set to  $c_1 = 121 \times 10^3 \text{ J m}^{-3}$ ,  $D_1 = 22.9 \times 10^3 \text{ J m}^{-3}$ ,  $D_1^{(2)} = 3.5 \times 10^3 \text{ J m}^{-3}$ ,  $D_1^{(3)} = 0.9 \times 10^3 \text{ J m}^{-3}$ ,  $D_2 = -42.0 \times 10^3 \text{ J m}^{-3}$ ,  $D_2^{nw} = -42.2 \times 10^3 \text{ J m}^{-3}$ ,  $D_2^{(2)} = -53.5 \times 10^3 \text{ J m}^{-3}$ , and  $D_2^{(2),nw} = -22.0 \times 10^3 \text{ J m}^{-3}$ . Here, the value of  $c_1$  follows

from a fit of the initial slope of the stress-strain curve resulting from the experimental data points. As explained above, the relationship between  $D_1$ ,  $D_2$ , and  $D_2^{nw}$  strongly influences the value of the threshold strain amplitude at which the reorientation of the director starts.  $D_1^{(2)}$  and  $D_1^{(3)}$  affect the length of the reorientation interval and the shape of the curve during this interval to a large extent. The same is true for  $D_2^{(2)}$  and  $D_2^{(2),nw}$ , whereas  $D_2$  and  $D_2^{nw}$  mainly influence the shape of the curve. As has already been mentioned above, the relative rotations  $\tilde{\Omega}^{nw}$  and therefore the values of the material parameters  $D_2^{nw}$  and  $D_2^{(2),nw}$  strongly affect the magnitude of the lateral contractions. We have carefully adjusted the values of the material parameters. However, small deviations from these values qualitatively lead to the same results.

Finally, we note that the slope of the stress-strain curve for high strain amplitudes is lower than for small strain amplitudes. This means that the generalized energy of the system increases less with increasing strain. If this were not the case, there would be no reason for the director to remain in the re-oriented position.

#### IV. DISCUSSION AND PERSPECTIVE

In this paper we have presented a continuum model which allows the description of the nonlinear macroscopic behavior of nematic SCLSEs. We propose that two preferred directions  $\hat{n}$  and  $\hat{n}^{nw}$  are important for the characterization of the materials, one of them connected to the properties of the liquid crystalline phase and the other one to the elastic behavior. From these two preferred directions, two sets of relative rotations  $\tilde{\Omega}$  and  $\tilde{\Omega}^{nw}$  arise. We have shown that for small deviations from the energetic ground state this picture is consistent with the previous characterization of the materials using only one set of relative rotations. Furthermore, we have demonstrated that the experimentally observed process of director reorientation and the connected decrease in the slope of the stress-strain curves can be described by our model. In this context, we have explained that the two sets of relative rotations  $\tilde{\Omega}$  and  $\tilde{\Omega}^{nw}$  are necessary so that the overall behavior of the materials can be recovered correctly. In addition, we have pointed out that one has to take into account explicitly the contribution of the nonlinear elastic behavior of the materials which is not connected to any reorientation of the director field. This plays a significant role for the interpretation of the stress-strain curves.

From our investigations, it is difficult to judge to what degree the shear described by  $S \neq 0$  may be observed for a volume element which behaves in a representative way. We have found that both a deformation without shear  $S = 0$  as well as a deformation including the shear  $S \neq 0$  can qualitatively reproduce the stress-strain behavior observed in the experiments. When we allow for a shear deformation  $S \neq 0$  to occur, the interval of the stress-strain curve with lower slope increases, or in other words, the strain interval during which the director reorients becomes larger. On the other hand we have demonstrated that the length of this interval is closely

connected to the influence of nonlinear terms coupling strain to relative rotations (in our case the terms with the coefficients  $D_2^{(2)}$  and  $D_2^{nw,(2)}$ ). There is a clear tendency that more nonlinear terms of this kind further increase the length of the reorientation interval. Accordingly, the observed stress-strain curve could also be modeled by a deformation of  $S = 0$ .

On the whole we will probably find a mixture of the two scenarios and intermediate states. We have to be aware, that the materials which are produced by the common techniques show a large degree of spatial inhomogeneities. Already by optical investigation one usually can detect some of these heterogeneities. Furthermore, also recent studies using NMR and calorimetry measurements revealed the same scenario on a different length scale<sup>40,41</sup>. Due to these inhomogeneities and the interaction of the various volume elements in the polymer material, we will find an elastic deformation which is to a large degree spatially heterogeneous. In addition, the boundary conditions of clamping the material induce further inhomogeneities in the deformation. Therefore, a macroscopically observed strain behavior will always be an average over varying strain behavior across the whole sample.

As a consequence, we must conclude that the degree of elastic shear deformation of one volume element does not only result strictly from minimizing its generalized energy. It seems to be more likely that the shear deformation is predominantly imposed onto the respective volume element by spatially inhomogeneous deformations. The local, spatially varying strain deformations have to arrange themselves in a way such that for the clamped edges of the elastomer we find the macroscopic displacement imposed from outside. However, we have shown that both for suppressed shear deformation  $S = 0$  as well as for the energetically favored shear deformation  $S \neq 0$  the stress-strain curves can qualitatively be reproduced.

Next, concerning the original data points in Fig. 3, reproduced from Ref. 29, we would like to compare the final slope for high strain amplitudes to the initial slope at low strains. We find approximately the same value for the two slopes, although the elastomer is stretched perpendicularly to the director in the beginning and in parallel direction at the end. Consequently, we may conclude that the overall elastic behavior of the sample is virtually isotropic with respect to the orientation of the director field. This justifies our choice of the elastic part of the generalized energy density (7), in which we neglected anisotropic elastic terms. The remaining difference between the initial and final slope of the curves in Fig. 5 can be explained by the influence of the relative rotations.

It is very important to address the slope of the data points in Fig. 5 for intermediate strain amplitudes as well. Here, we find a negative slope. On the contrary, we find a pronounced positive slope when we look at the overall stress-strain curves in Figs. 3 and 4. This means that in the regime of intermediate strain amplitudes the elastomer gains energy due to the reorientation of the director field on increasing strain deformation. However, during every step of increasing the strain, the intrinsic nonlinear part of the purely elastic deformation of the network of polymer backbones costs more energy than is gained from the process of director reorientation. Therefore,

the slope of the overall stress-strain curve is positive. We have also analyzed other recently measured stress-strain data in the same way<sup>30</sup>, and we have qualitatively obtained the same results.

We conclude that the underlying nonlinear elastic behavior of the network of polymer backbones can to a great extent be separated from the reorientation process. However, it has a major influence on the overall appearance of the stress-strain data. It prevents a plateau-like zero-slope intermediate region of the stress-strain curves. Due to its dominant contribution, it also seems to be justified to break down the interpretation of the stress-strain data to the spatially homogeneous behavior of one representative volume element: the nonlinear elastic behavior can mainly be attributed to every volume element of the material as a local effect, which does not arise from the nonlocal interaction of the different volume elements. The experimental data which we have selected in order to test our model clearly show this trend.

Possibly, oriented elastomer films in which this nonlinear elastic behavior plays a less dominant role can be produced. In this case, spatial heterogeneities become important for the macroscopic response of the system, and the interaction between different volume elements is certainly essential. Scenarios similar to those found for polydomain samples may occur<sup>42</sup>. Then the connection between the homogeneous behavior of one volume element and the overall behavior of the whole elastomer becomes a challenging problem. Phenomenologically, it may be attacked by an averaging approach in a spirit similar to a Maxwell construction. These issues can be investigated in future studies on the basis of our model.

## ACKNOWLEDGMENTS

The authors thank Kenji Urayama for stimulating discussions and for providing the values of the data points of the stress-strain curve. Furthermore, the authors thank Philippe Martinoty for stimulating discussions. A. M. M. thanks Professor DeSimone for a stimulating discussion on relative rotations. A. M. M. and H. R. B. thank the Deutsche Forschungsgemeinschaft through the Forschergruppe FOR608 ‘Nicht-lineare Dynamik komplexer Kontinua’ and the Deutscher Akademischer Austauschdienst (312/pro-ms) through PROCOPE for partial support of this work. A. M. M. thanks the Japan Society for the Promotion of Science for partial support of this work through a JSPS Fellowship.

## APPENDIX: SYMMETRY RELATIONS AND AN ALTERNATIVE DEFINITION OF RELATIVE ROTATIONS

In this appendix we discuss an alternative definition of the variables of relative rotations, which also takes into account the presence of the two preferred directions in nematic SCLSCEs. We demonstrate that this alternative definition leads to the same expression of the generalized energy density that we derived in section II and used in section III in order to characterize the behavior of the materials.

Talking about the variables of relative rotations, it might be more suggestive at a first glance to start the construction of the macroscopic variables with a rotation matrix. In our case, the matrix should describe the rotation of the direction given by  $\hat{\mathbf{n}}^{\text{nw}}$  to the direction given by  $\hat{\mathbf{n}}$ . We call this matrix  $\mathbf{W}$ .

In general, two spaces must be thought of in order to statically describe a distorted material. One is connected to the initial, undistorted state and may be called the initial space, the other one is connected to the distorted state and may be called final space<sup>36,37</sup>. Symmetry transformations in one of the two spaces do not imply the respective transformations in the other space. For example, this means that the transformation  $\hat{\mathbf{n}}_0 \rightarrow -\hat{\mathbf{n}}_0$ , which takes place in the initial space, does not imply  $\hat{\mathbf{n}} \rightarrow -\hat{\mathbf{n}}$  in the final space, and vice versa. The same is true for  $\hat{\mathbf{n}}_0^{\text{nw}}$  and  $\hat{\mathbf{n}}^{\text{nw}}$ .

We can see from definition (4) that  $\mathbf{S}$  is odd under the symmetry transformations  $\hat{\mathbf{n}}_0 \leftrightarrow -\hat{\mathbf{n}}_0$  and  $\hat{\mathbf{n}} \leftrightarrow -\hat{\mathbf{n}}$ , separately. From definition (5) we infer that  $\mathbf{R}$  is odd under the symmetry transformations  $\hat{\mathbf{n}}_0^{\text{nw}} \leftrightarrow -\hat{\mathbf{n}}_0^{\text{nw}}$  and  $\hat{\mathbf{n}}^{\text{nw}} \leftrightarrow -\hat{\mathbf{n}}^{\text{nw}}$ , separately. A rotation matrix  $\mathbf{S} \cdot \mathbf{R}$  describes how a direction parallel to  $\hat{\mathbf{n}}^{\text{nw}}$  is rotated to a direction parallel to  $\hat{\mathbf{n}}$ , however, this product matrix is odd under  $\hat{\mathbf{n}}_0 \leftrightarrow -\hat{\mathbf{n}}_0$ ,  $\hat{\mathbf{n}}_0^{\text{nw}} \leftrightarrow -\hat{\mathbf{n}}_0^{\text{nw}}$ ,  $\hat{\mathbf{n}} \leftrightarrow -\hat{\mathbf{n}}$ , and  $\hat{\mathbf{n}}^{\text{nw}} \leftrightarrow -\hat{\mathbf{n}}^{\text{nw}}$ , separately. In order to set up a hydrodynamic-like, Eulerian picture the variables must be independent of the initial space. Formally, we thus have to insert an additional matrix that transforms  $\hat{\mathbf{n}}_0^{\text{nw}}$  into  $\hat{\mathbf{n}}_0$  according to  $\hat{\mathbf{n}}_0 = \mathbf{T} \cdot \hat{\mathbf{n}}_0^{\text{nw}}$ , so that we define  $\mathbf{W} = \mathbf{S} \cdot \mathbf{T} \cdot \mathbf{R}$ .

$\mathbf{W}$  is the matrix we were looking for, which rotates  $\hat{\mathbf{n}}^{\text{nw}}$  to  $\hat{\mathbf{n}}$ . However, we cannot use the matrix  $\mathbf{W}$  directly as a macroscopic variable: as already mentioned in section II, in a hydrodynamic-like Eulerian picture the macroscopic variables contributing to the energy density must vanish when the system is in equilibrium and no external forces are applied. Subtracting unity from  $\mathbf{W}$  in order to satisfy this condition leads to problems, because  $\mathbf{W}$  is odd with respect to the transformations  $\hat{\mathbf{n}} \leftrightarrow -\hat{\mathbf{n}}$  and  $\hat{\mathbf{n}}^{\text{nw}} \leftrightarrow -\hat{\mathbf{n}}^{\text{nw}}$ , separately. Consequently, the resulting object would not have a clearly defined symmetry behavior under these transformations. The problem cannot be solved by simple projections as those which have led to the definitions (1) and (2).

We therefore propose a different approach. All the information stored in the rotation matrix  $\mathbf{W}$  is given by the direction of the rotation axis and the angle of rotation. However, the same information is also provided by the cross product of  $\hat{\mathbf{n}}^{\text{nw}}$  and  $\hat{\mathbf{n}}$ , so that, alternatively to Eqs. (1) and (2), in this appendix we define as variables of relative rotations

$$\tilde{\Omega}^{\text{alt}} := \hat{\mathbf{n}}^{\text{nw}} \times \hat{\mathbf{n}}. \quad (30)$$

Here, “ $\times$ ” denotes the cross product. Consequently, introducing the Levi-Civita tensor  $\epsilon_{ijk}$ , the components of  $\tilde{\Omega}^{\text{alt}}$  read

$$\tilde{\Omega}_i^{\text{alt}} = \epsilon_{ijk} n_j^{\text{nw}} n_k. \quad (31)$$

If we use this definition of the relative rotations, we can show that expression (7) for the generalized energy density  $F$  is obtained identically.

It is straightforward to verify that

$$\tilde{\Omega}_i \tilde{\Omega}_i = \tilde{\Omega}_i^{\text{nw}} \tilde{\Omega}_i^{\text{nw}} = \tilde{\Omega}_i^{\text{alt}} \tilde{\Omega}_i^{\text{alt}}. \quad (32)$$

For this reason, the terms in  $F$  with the coefficients  $D_1$ ,  $D_1^{(2)}$ , and  $D_1^{(3)}$  are recovered.

Coupling  $\tilde{\Omega}^{\text{alt}}$  to the strain  $\varepsilon$  in lowest order and respecting the symmetry behavior of  $F$  leads to two terms

$$\begin{aligned} n_i \varepsilon_{ij} \varepsilon_{jkl} n_k^{nw} \tilde{\Omega}_l^{\text{alt}} &= - [n_i \varepsilon_{ij} n_j - n_i \varepsilon_{ij} n_j^{nw} (n_k n_k^{nw})] \\ &= - n_i \varepsilon_{ij} \tilde{\Omega}_j \end{aligned} \quad (33)$$

and

$$\begin{aligned} n_i^{nw} \varepsilon_{ij} \varepsilon_{jkl} n_k \tilde{\Omega}_l^{\text{alt}} &= n_i^{nw} \varepsilon_{ij} n_j^{nw} - n_i \varepsilon_{ij} n_j (n_k n_k^{nw}) \\ &= - n_i^{nw} \varepsilon_{ij} \tilde{\Omega}_j^{nw}. \end{aligned} \quad (34)$$

They correspond to the terms with the coefficients  $D_2$  and  $D_2^{nw}$  in the generalized energy density  $F$ . The terms with the coefficients  $D_2^{(2)}$  and  $D_2^{nw,(2)}$  are obtained in the same way.

Therefore, a characterization of the materials by the two definitions of relative rotations (1) and (2) on the one hand, and (30) on the other hand are identical as long as we confine ourselves to the terms listed in expression (7). In particular, the analysis presented in section III would be the same if one uses as an alternative definition of relative rotations expression (30).

- 
- <sup>1</sup> J. Küpfer and H. Finkelmann, *Makromol. Chem., Rapid Commun.* **12**, 717 (1991).  
<sup>2</sup> J. Küpfer and H. Finkelmann, *Macromol. Chem. Phys.* **195**, 1353 (1994).  
<sup>3</sup> I. Kundler and H. Finkelmann, *Macromol. Rapid Commun.* **16**, 679 (1995).  
<sup>4</sup> I. Kundler and H. Finkelmann, *Macromol. Chem. Phys.* **199**, 677 (1998).  
<sup>5</sup> K. Urayama, S. Honda, and T. Takigawa, *Macromol.* **38**, 3574 (2005).  
<sup>6</sup> Y. Yusuf, J. H. Huh, P. E. Cladis, H. R. Brand, H. Finkelmann, and S. Kai, *Phys. Rev. E* **71**, 061702 (2005).  
<sup>7</sup> D.-U. Cho, Y. Yusuf, P. E. Cladis, H. R. Brand, H. Finkelmann, and S. Kai, *Jap. J. Appl. Phys.* **46**, 1106 (2007).  
<sup>8</sup> M. Warner and E. M. Terentjev, *Liquid Crystal Elastomers* (Clarendon Press, Oxford, 2003); and references therein.  
<sup>9</sup> S. Conti, A. DeSimone, and G. Dolzmann, *J. Mech. Phys. Solids* **50**, 1431 (2002).  
<sup>10</sup> D. Rogez, G. Francius, H. Finkelmann, and P. Martinoty, *Eur. Phys. J. E* **20**, 369 (2006).  
<sup>11</sup> P. Martinoty, P. Stein, H. Finkelmann, H. Pleiner, and H. R. Brand, *Eur. Phys. J. E* **14**, 311 (2004).  
<sup>12</sup> H. R. Brand, H. Pleiner, and P. Martinoty, *Soft Matter* **2**, 182 (2006).  
<sup>13</sup> L. Golubović and T. C. Lubensky, *Phys. Rev. Lett.* **63**, 1082 (1989).  
<sup>14</sup> F. Ye, R. Mukhopadhyay, O. Stenull, and T. C. Lubensky, *Phys. Rev. Lett.* **98**, 147801 (2007).  
<sup>15</sup> E. Fried and S. Sellers, *J. Mech. Phys. Solids* **52**, 1671 (2004).  
<sup>16</sup> E. Fried and S. Sellers, *J. Appl. Phys.* **100**, 043521 (2006).  
<sup>17</sup> P. G. de Gennes, in *Liquid Crystals of One- and Two-Dimensional Order*, edited by W. Helfrich and G. Heppke (Springer, Berlin, 1980), p. 231.  
<sup>18</sup> H. R. Brand and H. Pleiner, *Physica A* **208**, 359 (1994).  
<sup>19</sup> J. Weilepp and H. R. Brand, *Europhys. Lett.* **34**, 495 (1996).  
<sup>20</sup> O. Müller and H. R. Brand, *Eur. Phys. J. E* **17**, 53 (2005).  
<sup>21</sup> A. M. Menzel and H. R. Brand, *Eur. Phys. J. E* **26**, 235 (2008).  
<sup>22</sup> A. M. Menzel, H. Pleiner, and H. R. Brand, *J. Chem. Phys.* **126**, 234901 (2007).  
<sup>23</sup> P. G. de Gennes, M. Hébert, and R. Kant, *Macromol. Symp.* **113**, 39 (1997).  
<sup>24</sup> M. Hébert, R. Kant, and P. G. de Gennes, *J. Phys.* **17**, 909 (1997).  
<sup>25</sup> Y. Yu and T. Ikeda, *Angew. Chem. Int. Ed.* **45**, 5416 (2006).  
<sup>26</sup> A. Cho, *Science* **287**, 783 (2000); R. Pelrine, R. Kornbluh, Q. Pei, and J. Joseph, *Science* **287**, 836 (2000).  
<sup>27</sup> F. Vollrath and D. P. Knight, *Nature* **410**, 541 (2001); and references therein.  
<sup>28</sup> G. R. Plaza, G. V. Guinea, J. Pérez-Rigueiro, and M. Elices, *J. Polym. Sci. B* **44**, 994 (2006).  
<sup>29</sup> K. Urayama, R. Mashita, I. Kobayashi, and T. Takigawa, *Macromol.* **40**, 7665 (2007).  
<sup>30</sup> F. Brömmel and H. Finkelmann (unpublished).  
<sup>31</sup> H. R. Brand, K. Kawasaki, *Macromol. Rapid Commun.* **15**, 251 (1994).  
<sup>32</sup> C. H. Legge, F. J. Davis, and G. R. Mitchell, *J. Phys. II (France)* **1**, 1253 (1991).  
<sup>33</sup> S. T. Kim and H. Finkelmann, *Macromol. Rapid Commun.* **22**, 429 (2001).  
<sup>34</sup> A. Komp, J. Rühle, and H. Finkelmann, *Macromol. Rapid Commun.* **26**, 813 (2005).  
<sup>35</sup> More precisely, a so-called initial field  $\mathbf{a}(\mathbf{r})$  must be used in an Eulerian description instead of the displacement field  $\mathbf{u}(\mathbf{r})$ <sup>36,37</sup>. However, in a static picture, we can also perform our analysis in terms of  $\mathbf{u}(\mathbf{r})$ .  
<sup>36</sup> H. Temmen, H. Pleiner, M. Liu, and H. R. Brand, *Phys. Rev. Lett.* **84**, 3228 (2000).  
<sup>37</sup> H. Pleiner, M. Liu, and H. R. Brand, *Rheol. Acta* **39**, 560 (2000).  
<sup>38</sup> L. R. G. Treloar, *The Physics of rubber elasticity* (Clarendon Press, Oxford, 1975).  
<sup>39</sup> G. R. Mitchell, F. J. Davis, and W. Guo, *Phys. Rev. Lett.* **71**, 2947 (1993).  
<sup>40</sup> A. Lebar, Z. Kutnjak, S. Žumer, H. Finkelmann, A. Sánchez-Ferrer, and B. Zalar, *Phys. Rev. Lett.* **94**, 197801 (2005).  
<sup>41</sup> G. Cordoyiannis, A. Lebar, B. Zalar, S. Žumer, H. Finkelmann, and Z. Kutnjak, *Phys. Rev. Lett.* **99**, 197801 (2007).  
<sup>42</sup> N. Uchida, *Phys. Rev. E* **60**, R13 (1999).